

Comparative Analysis of Poincare Solutions of Harmonically Excited Duffing Oscillator Using Fractal Characterization

Salau, T.A.O.¹, Olopade, T.I.²

Department of Mechanical Engineering, University of Ibadan, Oyo state, Nigeria.

ABSTRACT: This paper adopted five popular Runge-Kutta algorithms ranging from order two to five as well as modified order five to investigate the chaotic behavior of the excited Duffing Oscillator using fractal disk dimension characterization. Studied nodal points included 11×11 to 101×101 at a step increment of 10 along each of the excitation amplitude and damping coefficient axes and for three equilibrium positions: $(-1,0)$, $(0,0)$ and $(1,0)$. Excitation amplitude and damping co-efficient range are $0.10 \leq P_o \leq 0.21$ and $0.0168 \leq \gamma \leq 0.168$ respectively. Common parameters to all studied cases included the excitation frequency(1.0) and random number generating seed value of 9876. The probability that any combination of parameters selected at random from within the studied parameter plane can drive the Duffing Oscillator chaotically was obtained to be 62.63%, 58.58%, 63.53% for the respective equilibrium positions $(-1,0)$, $(0,0)$ and $(1,0)$ using the popular fourth order scheme. This probability measure was found to be insignificantly different quantitatively for the remaining four schemes studied.

Keywords: Duffing Oscillator, Damping co-efficient, Excitation Amplitude, Runge-Kutta schemes, Fractal disk dimension.

I. INTRODUCTION

The Duffing oscillator has been described physically as an oscillator with a restoring spring force which does not obey Hooke's law. The Duffing Equation was named after the German electrical engineer Georg Duffing in 1918. It is undoubtedly one of the most intensively studied systems in dynamics, and it found its application as models of various physical and engineering situations such as Josephon junctions, optical bistability, plasma oscillators, buckled beams of plate under transverse dynamic excitation, ship dynamics, vibration isolators and electrical circuits [1]. A common model using this oscillator involves an electro-magnetized vibrating beam analyzed as exhibiting cusp catastrophic behavior for certain parameter values [2]. The physical model depicts the Duffing Oscillator as two magnets that deflect a steel beam toward each other as shown in figure 1.

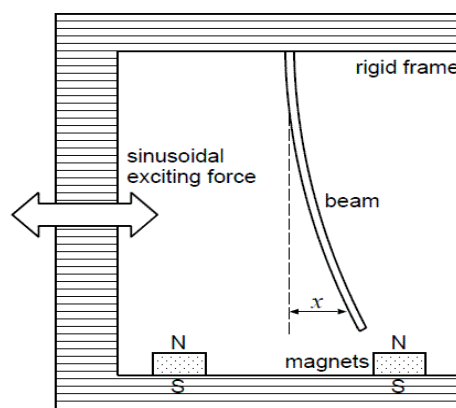


Figure 1: The physical model of the Duffing Oscillator.

The Duffing Oscillator has gained wide applications in the field of engineering, medicine, economics, weather forecast, biology. Research article [3] modelled the dynamics of a ship by modifying the Duffing's equation and using the oscillation of sea waves as the parameter, while [4] established that the deterministic

Duffing-Oscillator-Model (DOM) is suitable for examining inventory fluctuations of wheat in the global market for a given time period, with reasonable credibility. In such problems which are modelled mathematically from physical problems, initial conditions usually have very tangible interpretations for differential equations derived from physical problem settings.

It was concluded by [5] that the Duffing equation behaves interestingly and begins to show chaotic behavior at excitation amplitude of $P_0=0.21$, damping coefficient, $\gamma=0.168$ and a forcing frequency of $\omega=1.0$. He further noticed that at other conditions fixed, that when the excitation amplitude varies between $0 \leq P_0 \leq 0.177$, the system responded by oscillating through one period as the force also oscillates through one period (one period motion), and at $P_0=0.178$, the system oscillates through one-half a period as the force oscillates through a period which implies that for the response to go through a period, the force must oscillate through two periods. This has led to the study of the Duffing Oscillator and different modified Duffing Oscillators to suit different applications by different authors.

Research article [6] studied the Duffing Oscillator and were able to demonstrate visual comparisons of the chaotic behavior of the Duffing Oscillator in the plane of the excitation amplitude versus the forcing frequency using adaptive time steps Runge-Kutta fourth and fifth order algorithms to compute simultaneously multiple trajectories of a harmonically excited Duffing oscillator from very close initial conditions. It was obtained from the study, that the chances of chaotic behavior were higher for combined higher excitation amplitudes and frequencies alongside smaller damp coefficient.

Research article [7] proceeded to further adopt two popular Runge-Kutta algorithms (fourth and fifth orders) to investigate the chaotic driven impact of both the damp coefficient and the excitation amplitude on the Duffing Oscillator. The study was able to identify and support damp parameter proper tuning as an easier agent of impacting chaotic behavior in Duffing Oscillator compared with the excitation amplitude provided other simulation conditions remain the same while this study utilizes five popular Runge-Kutta algorithms to investigate the Duffing Oscillator in the plane of excitation amplitude and the damping coefficient.

II. METHODOLOGY

This research studied the normalized governing equation of harmonically excited Duffing system given in the equation below with reference to [5], [8] and [9].

$$\ddot{x} + \gamma \dot{x} - \frac{x}{2}(1-x) = P_0 \sin(\omega t) \dots \dots \dots (1)$$

In equation (1), x , \dot{x} and \ddot{x} represents respectively displacement, velocity and acceleration of the oscillator about a set equilibrium position. By damp and harmonic excitation, it means that the system is controlled by a sinusoidally varying load with an amplitude strength, damp coefficient, frequency and time given respectively as: P_0, γ, ω and t . According to literature, combination of $\gamma = 0.168$, $P_0 = 0.21$, and $\omega = 1.0$ or $\gamma = 0.0168$, $P_0 = 0.09$ and $\omega = 1.0$ parameters leads to chaotic behavior which were validated with the Poincare section obtained using these parameters [5]. However, this study focuses on the comparison of solutions obtained using the second to fifth, as well as modified fifth orders Runge-Kutta simulations at different resolutions in the plane of the excitation amplitude and damping coefficient and equilibrium positions as described later. The scattered Poincare plots of simulation obtained for the excited Duffing oscillator were captured and characterised using fractal disk dimension obtained by optimum disk count method of [10]. The relative distribution of the fractal disk dimensions were obtained and compared over one hundred subintervals for the cases and simulation algorithms. Thereafter, error analyses and variation for schemes and drive parameters were performed and the results were interpreted. The schemes were then paired and correlation analysis was performed over range of drive parameters and the findings were interpreted.

III. PARAMETER DETAILS OF STUDIED CASES

A case is defined as a point on the parameter plane. 11×11 up to 101×101 cases were studied at fixed excitation frequency alongside ten different constant step incremental of damping coefficient ($0.0168 \leq \gamma \leq 0.1680$) and excitation amplitude ($0.10 \leq P_0 \leq 0.21$) over large number of excitation period at the equilibrium position (0,0). Then 101×101 cases were also examined at a constant step incremental of damping coefficient ($0.0168 \leq \gamma \leq 0.1680$) and excitation amplitude ($0.10 \leq P_0 \leq 0.21$), over large number of excitation period at the equilibrium positions (1,0) and (-1,0). Common parameters to all cases include the excitation frequency value, $\omega=1.0$ and random number generating seed value of 9876. A typical parameter plane is shown in figure 2.

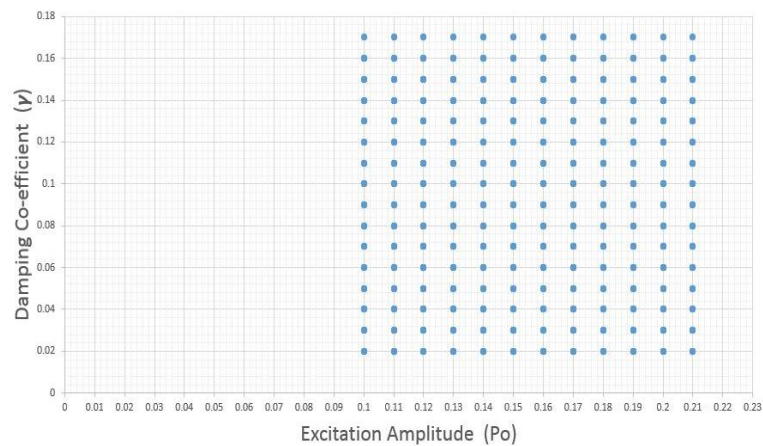


Figure 2: Parameter space for excitation amplitude and the damping coefficient ranging from $0.10 \leq P_o \leq 0.21$ and $0.0168 \leq \gamma \leq 0.168$ respectively.

IV. POINCARÉ SOLUTIONS

The phase space trajectory of the motion for all time is called the phase plot out of which the Poincaré solutions is filtered out. Rather than considering the phase space trajectory for all times, which gives a continuous curve, a discrete set of phase space points of the particle at every period of the driving force, i.e. when time $(t) = 2\pi/\omega, 4\pi/\omega, 6\pi/\omega$, etc could be considered. The resulting image of the collection of displacement and velocity components as scattered plot for all these discrete times is referred to as Poincaré section. It is a periodical collection of fundamental solutions obtained for a dynamical system. That is other solutions are available at every point in time, since time never stops, but our focus of interest is at a certain point in time which occurs at a constant interval of the period of the exciting force. Thus, embedded in a single phase plot are numerous scattered plot which varies by the time step or interval used. Clearly for a periodic orbit the Poincaré section is a single point, when the period has doubled it consists of two points, when the period triple, it consist of three points and so on. The Poincaré sections obtained are termed attractors. A typical Duffing attractor obtained at $P_o=0.21, \gamma=0.168, \omega=1.0$ using the order five modified scheme is shown in figure 3.

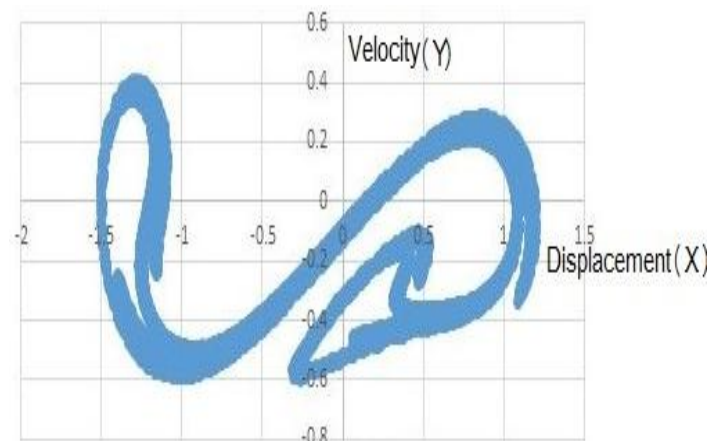


Figure 3: Poincaré maps of the Duffing equation using $P_o=0.21, \gamma=0.168, \omega=1.0$ obtained using the order five modified scheme.

V. ATTRACTOR CHARACTERIZATION

The optimum disk count algorithm was employed in charactering all the resulting attractors based on ten (10) different disk scales of examination and over five (5) independent trials. The Duffing oscillator was considered to have behaved chaotically when the estimated disk dimension is greater than zero and non-chaotic at an estimated disk dimension of zero.

VI. RESULTS AND DISCUSSION

The Poincare sections were simulated and the corresponding fractal dimensions were estimated. A typical fractal dimensions obtained during one of the simulation is given in table I.

Table I: Selected Cases of Variation of the Estimated Fractal Disk Dimension of Poincare Section with Simulation Schemes using Constant Time Step obtained across 121 nodal simulations at the equilibrium position (0,0)

Po	γ	RK2-D2	RK3-D3	RK4-D4	RK5-D5	RK5M-D5M
0.1000	0.0168	1.14	1.07	1.18	1.22	0.77
0.1000	0.0319	0.80	0.71	0.95	0.97	1.42
0.1000	0.0470	0.77	0.82	0.78	0.88	0.82
0.1000	0.0622	0.76	0.82	0.96	0.99	1.07
0.1000	0.0773	0.00	0.00	0.00	0.00	0.00
0.1000	0.0924	0.00	0.00	0.00	0.00	0.00
0.1000	0.1075	0.00	0.00	0.00	0.00	0.00
0.1000	0.1226	0.00	0.00	0.00	0.00	0.00
0.1000	0.1378	0.00	0.00	0.00	0.00	0.00
0.1000	0.1529	0.00	0.00	0.00	0.00	0.00
0.1000	0.1680	0.00	0.00	0.00	0.00	0.00
0.1110	0.0168	1.16	0.52	1.01	1.35	1.58
0.1110	0.0319	1.01	0.86	1.02	0.99	1.02
0.1110	0.0470	0.53	0.70	0.70	0.72	0.69
0.1110	0.0622	0.17	0.00	0.00	0.00	0.00
0.1110	0.0773	0.00	0.00	0.00	0.00	0.00
0.1110	0.0924	0.00	0.00	0.00	0.00	0.00
0.1110	0.1075	0.00	0.00	0.00	0.00	0.00
0.1110	0.1226	0.00	0.00	0.00	0.00	0.00
0.1110	0.1378	0.00	0.00	0.00	0.00	0.00
0.1110	0.1529	0.00	0.00	0.00	0.00	0.00
0.1110	0.1680	0.00	0.00	0.00	0.00	0.00
0.1220	0.0168	1.67	1.63	1.65	1.60	1.56
0.1220	0.0319	0.13	0.13	0.13	0.13	0.13
0.1220	0.0470	0.00	0.00	0.00	0.00	0.00
0.1220	0.0622	0.00	0.00	0.00	0.00	0.00
0.1220	0.0773	0.00	0.00	0.00	0.00	0.00
0.1220	0.0924	0.00	0.00	0.00	0.00	0.00
0.1220	0.1075	0.00	0.00	0.00	0.00	0.00
0.1220	0.1226	0.00	0.00	0.00	0.00	0.00
0.1220	0.1378	0.00	0.00	0.00	0.00	0.00
0.1220	0.1529	0.00	0.00	0.00	0.00	0.00
0.1220	0.1680	0.00	0.00	0.00	0.00	0.00
0.1330	0.0168	0.80	1.37	1.68	1.60	1.62
0.1330	0.0319	1.57	1.57	1.61	1.61	1.58
0.1330	0.0470	1.52	1.48	1.10	1.60	1.45
0.1330	0.0622	1.37	1.34	1.43	1.35	1.31
0.1330	0.0773	0.52	0.45	0.45	0.45	0.45
0.1330	0.0924	0.00	0.08	0.08	0.08	0.08
0.1330	0.1075	0.00	0.00	0.00	0.00	0.00
0.1330	0.1226	0.00	0.00	0.00	0.00	0.00
0.1330	0.1378	0.00	0.00	0.00	0.00	0.00
0.1330	0.1529	0.00	0.00	0.00	0.00	0.00
0.1330	0.1680	0.00	0.00	0.00	0.00	0.00
0.1440	0.0168	0.86	0.83	0.83	0.84	0.84

Table I Continued: Selected Cases of Variation of the Estimated Fractal Disk Dimension of Poincare Section with Simulation Schemes using Constant Time Step obtained across 121 nodal simulations at the equilibrium position (0,0).

0.1440	0.0319	1.37	1.28	1.37	0.86	0.83
0.1440	0.0470	0.87	0.63	0.62	0.80	0.76
0.1440	0.0622	0.98	0.62	1.31	1.27	1.04
0.1440	0.0773	1.28	0.00	0.00	1.11	1.19
0.1440	0.0924	0.00	0.00	0.00	0.70	0.66
0.1440	0.1075	0.00	0.00	0.00	0.00	0.00
0.1440	0.1226	0.00	0.90	0.55	1.08	0.47
0.1440	0.1378	0.00	0.00	0.00	0.00	0.00
0.1440	0.1529	0.00	0.00	0.00	0.00	0.00
0.1440	0.1680	0.00	0.00	0.00	0.00	0.00
0.1550	0.0168	1.72	0.91	1.65	1.67	1.40
0.1550	0.0319	1.63	1.11	0.68	0.81	1.53
0.1550	0.0470	0.82	0.61	1.41	0.84	0.49
0.1550	0.0622	0.75	0.84	1.21	1.42	0.71
0.1550	0.0773	1.20	0.56	0.76	0.00	1.26
0.1550	0.0924	0.00	0.00	0.00	0.00	0.00
0.1550	0.1075	0.55	0.92	1.30	0.98	0.59
0.1550	0.1226	1.02	0.00	0.00	0.00	0.00
0.1550	0.1378	0.00	0.12	1.03	0.17	0.77
0.1550	0.1529	0.00	0.00	0.00	0.00	0.00
0.1550	0.1680	0.00	0.00	0.00	0.00	0.00
0.1660	0.0168	1.74	1.72	1.67	1.74	1.71
0.1660	0.0319	1.43	1.59	1.31	0.13	1.65
0.1660	0.0470	0.82	1.36	1.44	1.33	0.10
0.1660	0.0622	1.17	1.39	0.92	0.01	0.00
0.1660	0.0773	0.00	0.00	0.00	0.00	0.00
0.1660	0.0924	0.11	0.21	0.21	0.21	0.21
0.1660	0.1075	0.36	0.40	0.40	0.40	0.40
0.1660	0.1226	0.64	0.00	0.00	0.00	0.00
0.1660	0.1378	0.00	0.00	0.00	0.00	0.00
0.1660	0.1529	0.00	0.00	0.00	0.00	0.00
0.1660	0.1680	0.00	0.00	0.00	0.00	0.00
0.1770	0.0168	1.74	1.67	1.72	1.66	1.72
0.1770	0.0319	1.66	1.58	0.35	1.68	1.36
0.1770	0.0470	1.63	1.63	1.58	1.62	1.58
0.1770	0.0622	1.59	1.58	1.57	1.54	1.53
0.1770	0.0773	1.52	1.29	1.46	1.41	1.43
0.1770	0.0924	0.32	0.09	0.09	0.07	0.07
0.1770	0.1075	0.00	0.00	0.00	0.00	0.00
0.1770	0.1226	0.00	0.00	0.00	0.00	0.00
0.1770	0.1378	0.00	0.00	0.00	0.00	0.00
0.1770	0.1529	0.11	0.21	0.21	0.21	0.21
0.1770	0.1680	0.38	0.81	0.81	0.80	0.80
0.1880	0.0168	1.19	1.70	1.77	1.75	1.72
0.1880	0.0319	1.69	1.70	1.69	1.70	1.68
0.1880	0.0470	1.57	1.63	1.64	1.63	1.62
0.1880	0.0622	1.57	1.54	1.56	1.58	1.58

Table I Continued: Selected Cases of Variation of the Estimated Fractal Disk Dimension of Poincare Section with Simulation Schemes using Constant Time Step obtained across 121 nodal simulations at the equilibrium position (0,0).

0.1880	0.0773	1.50	1.54	1.53	1.49	1.53
0.1880	0.0924	1.49	1.46	1.44	1.47	1.47
0.1880	0.1075	0.79	0.66	0.97	1.02	0.43
0.1880	0.1226	0.84	0.37	1.05	0.37	1.13
0.1880	0.1378	0.35	0.31	0.31	0.31	0.31
0.1880	0.1529	0.00	0.00	0.00	0.00	0.00
0.1880	0.1680	0.00	0.00	0.00	0.00	0.00
0.1990	0.0168	1.44	1.51	1.48	1.53	1.54
0.1990	0.0319	1.70	1.71	1.68	1.68	1.66
0.1990	0.0470	1.67	1.66	1.60	1.62	1.61
0.1990	0.0622	1.60	1.57	1.57	1.56	1.57
0.1990	0.0773	1.54	1.53	1.54	1.55	1.54
0.1990	0.0924	1.53	1.49	1.52	1.49	1.50
0.1990	0.1075	1.45	1.46	1.45	1.41	1.45
0.1990	0.1226	0.32	0.99	0.37	0.37	0.37
0.1990	0.1378	0.76	0.89	1.29	1.33	1.07
0.1990	0.1529	1.32	1.34	1.31	1.32	1.35
0.1990	0.1680	0.55	0.29	0.29	0.29	0.29
0.2100	0.0168	1.36	1.20	1.36	1.19	1.16
0.2100	0.0319	1.70	1.71	1.70	1.62	1.67
0.2100	0.0470	1.68	1.61	1.65	1.68	1.64
0.2100	0.0622	1.60	1.55	1.59	1.59	1.60
0.2100	0.0773	1.54	1.56	1.56	1.53	1.55
0.2100	0.0924	1.52	1.51	1.50	1.51	1.52
0.2100	0.1075	1.45	1.47	1.48	1.43	1.47
0.2100	0.1226	1.25	0.29	0.32	0.32	0.52
0.2100	0.1378	0.66	1.06	1.32	1.05	1.01
0.2100	0.1529	1.37	1.37	1.38	1.38	1.40
0.2100	0.1680	1.35	1.34	1.37	1.32	1.34

With the criteria that an estimated fractal dimension above zero signifies chaos, the probabilities that the Duffing Oscillator will be driven chaotically when explored within the different resolution of the parameter space and at different resolutions are summarized in tables II and III. Table II shows the number of parameter set that drove the Duffing Oscillator chaotically as the nodal simulation increased and the initial condition (equilibrium position) of the system is maintained at (0,0), while table III reveals a similar information obtained at a constant nodal simulation but at three different equilibrium positions (-1,0), (0,0), (1,0). The chaotic parameters result reveals that the percentage of the chaotic parameters in the parameter space provided by all the Runge-Kutta schemes agree quantitatively well except for that provided by the second order Runge-Kutta scheme. Table II shows that the Duffing Oscillator is less driven chaotically at the equilibrium position (0,0), while it is observed to be more stable at the other two equilibrium positions (1,0) and (-1,0) since their percentage of chaotic parameters agree quantitatively well.

Table II: Percentage of chaotic parameter of the Duffing Oscillator across the various simulations at the equilibrium position (0,0)

No of Nodal Simulations	RK2	RK3	RK4	RK5	RK5M
11 X 11 =121	73 (60.34%)	72 (59.50%)	72 (59.50%)	73 (60.33%)	73 (60.33%)
21 X 21 =441	259 (58.73%)	259 (59.86%)	264 (59.41%)	259 (58.73%)	261 (59.18%)
31 X 31 =961	579 (60.25%)	565 (58.80%)	557 (57.96%)	566 (58.90%)	565 (58.80%)
41 X 41 =1681	1009 (60.02%)	986 (58.66%)	981 (58.36%)	973 (57.88%)	978 (58.18%)
51 X 51 =2601	1567 (60.25%)	1526 (58.67%)	1526 (58.67%)	1526 (58.67%)	1522 (58.52%)
61 X 61 =3721	2247 (60.39%)	2189 (58.83%)	2180 (58.59%)	2178 (58.53%)	2175 (58.45%)
71 X 71 =5041	3033 (60.17%)	2953 (58.85%)	2971 (58.94%)	2966 (58.84%)	2954 (58.60%)
81 X 81 =6561	3973 (60.55%)	3845 (58.60%)	3830 (58.38%)	3818 (58.19%)	3821 (58.24%)
91 X 91 =8281	5012 (60.52%)	4844 (58.50%)	4841 (58.46%)	4857 (58.65%)	4859 (58.68%)
101 X 101 =10201	6141 (60.20%)	5979 (58.61%)	5976 (58.58%)	5971 (58.53%)	5954 (58.37%)

Table III: Percentage of chaotic parameter of the Duffing Oscillator across the various simulations at the three equilibrium positions.

INITIAL CONDITION	No of Nodal Simulations	RK2	RK3	RK4	RK5	RK5M
X ₀₀ =1, Y ₀₀ =0	101 X 101 =10201	6662 (65.31%)	6504 (63.76%)	6481 (63.53%)	6502 (63.74%)	6494 (63.66%)
X ₀₀ =0, Y ₀₀ =0	101 X 101 =10201	6141 (60.20%)	5979 (58.61%)	5976 (58.58%)	5971 (58.53%)	5954 (58.37%)
X ₀₀ =-1, Y ₀₀ =0	101 X 101 =10201	6505 (63.77%)	6398 (62.72%)	6389 (62.63%)	6402 (62.76%)	6396 (62.70)

The correlation coefficient shows the degree of agreement of the two sets of data paired. It ranges between zero and one. A correlation coefficient value of 1.0 signifies total agreement between the set of data plotted while a value of zero means that there is no agreement at all between the two sets of data. Some of the correlation coefficients obtained are detailed in figures 4 and 5.

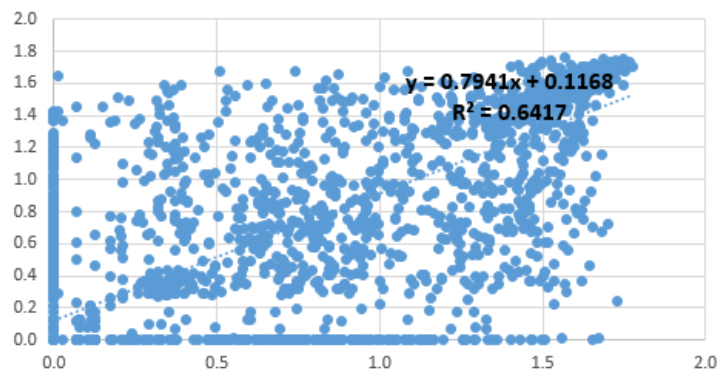


Figure 4: Correlation Plot of the Estimated Fractal Disk Dimension (EDD) by RK2 and RK4 with constant simulation time step for 50 by 50 resolutions

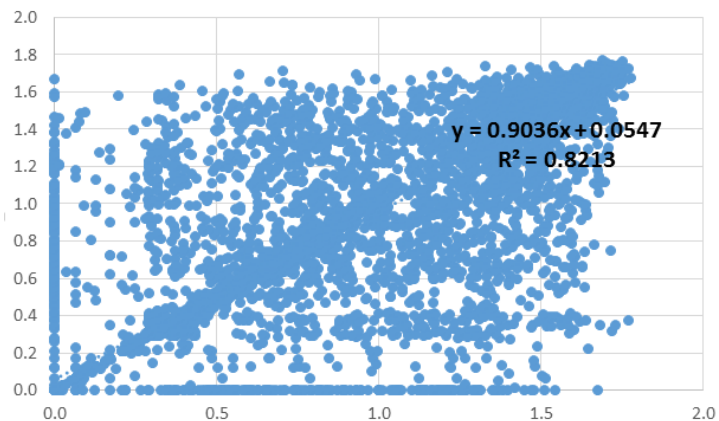


Figure 5: Correlation Plot of the Estimated Fractal Disk Dimension (EDD) by RK3 and RK5M with constant simulation time step for 100 by 100 resolutions.

The correlation coefficient of the estimated fractal disk dimension obtained by the second order Runge-Kutta scheme when paired with that obtained from the other schemes are low as revealed in tables IV and V.

Table IV: Correlation Analysis of Pairs of Runge-Kutta schemes at 2601 simulation points (51 by 51 nodes).

	RK2	RK3	RK4	RK5	RK5M
RK2	X	0.7686	0.7623	0.7530	0.7593
RK3		X	0.8730	0.8173	0.8188
RK4			X	0.8376	0.8236
RK5				X	0.8745
RK5M					X

Table V: Correlation Analysis of Pairs of Runge-Kutta schemes at 10201 simulation points(101 by 101 nodes).

	RK2	RK3	RK4	RK5	RK5M
RK2	X	0.7436	0.7466	0.7470	0.7434
RK3		X	0.8697	0.8183	0.8213
RK4			X	0.8236	0.8239
RK5				X	0.8769
RK5M					X

A careful observance of all the columns of table VI and VII shows that the first four rows of each column are the lowest set of correlation coefficient per column. This shows the disagreement of RK2 schemes with the other scheme. On the other hand, the highest value of the correlation coefficient occurs at the last row of each column showing the strong agreement between the estimated fractal disk dimension of the fifth order Runge-Kutta scheme and the modified fifth order Runge-Kutta scheme.

From tables VI and VII, using the fourth order Runge-Kutta scheme as the bench mark due to its speed and the reliability of its results, the third order ranks best among the remaining four Runge-Kutta algorithms with a correlation coefficient of 0.8227, 0.8697, and 0.8093 for case 1, case 2, and case 3 respectively. This implies that the third order Runge-Kutta scheme which takes lesser time to compute could also be employed in researching the Duffing Oscillator within the range of the drive parameters with little loss in accuracy of the results obtained.

Table VI: Correlation Analysis of Pairs of Runge-Kutta schemes at various nodal simulations.

X ₀₀ =0, Y ₀₀ =0										
NODES										
	11 X 11	21 X 21	31 X 31	41 X 41	51 X 51	61 X 61	71 X 71	81 X 81	91 X 91	101 X 101
PAIR OF SCHEMES	R-SQUARED VALUE									
RK2 - RK3	0.8365	0.7544	0.7687	0.7411	0.7686	0.7536	0.7500	0.7436	0.7386	0.7436
RK2 - RK4	0.7861	0.7465	0.7658	0.7411	0.7623	0.7522	0.7528	0.7497	0.7442	0.7466
RK2 - RK5	0.7821	0.7751	0.7322	0.7441	0.7530	0.7383	0.7426	0.7486	0.7452	0.7470
RK2 - RK5M	0.8509	0.7914	0.7592	0.7438	0.7593	0.7408	0.7311	0.7463	0.7527	0.7434
RK3 - RK4	0.8822	0.8643	0.8746	0.8711	0.8730	0.8803	0.8612	0.8687	0.8611	0.8697
RK3 - RK5	0.8357	0.7945	0.8368	0.8235	0.8173	0.8307	0.8167	0.8263	0.8098	0.8183
RK3 - RK5M	0.8168	0.7920	0.8365	0.8151	0.8188	0.8173	0.8099	0.8274	0.8123	0.8213
RK4 - RK5	0.8442	0.8094	0.8460	0.8308	0.8376	0.8316	0.8256	0.8285	0.8229	0.8236
RK4 - RK5M	0.8249	0.8095	0.8408	0.8235	0.8236	0.8176	0.8170	0.8262	0.8214	0.8239
RK5 - RK5M	0.8407	0.8668	0.8749	0.8814	0.8745	0.8699	0.8675	0.8818	0.8749	0.8769

Table VII: Correlation Analysis of Pairs of Runge-Kutta schemes at 10,201 simulations for the three equilibrium positions.

INITIAL CONDITION	X ₀₀ =0, Y ₀₀ = -1	X ₀₀ =0, Y ₀₀ =0	X ₀₀ =0, Y ₀₀ =1
101 X 101 NODES			
PAIR OF SCHEMES	R-SQUARED VALUE		
RK2 - RK3	0.6942	0.7436	0.6508
RK2 - RK4	0.6916	0.7466	0.6557
RK2 - RK5	0.6862	0.7470	0.6528
RK2 - RK5M	0.6908	0.7434	0.6463
RK3 - RK4	0.8227	0.8697	0.8093
RK3 - RK5	0.7594	0.8183	0.7369
RK3 - RK5M	0.7663	0.8213	0.7292
RK4 - RK5	0.7624	0.8236	0.7315
RK4 - RK5M	0.7584	0.8239	0.7341
RK5 - RK5M	0.8324	0.8769	0.8223

From tables VIII and IX, the higher coefficient of fitness ($R^2=0.80$) and slope value that is not less than 0.88 recorded between pairs of scheme from RK3, RK4, RK5 and RK5M are strong indicator that any of these schemes is good enough to simulate the Poincare section of the Duffing Oscillator with further processing or not.

Table VIII: Trend line parameter of correlation plot of the Estimated Fractal Disk Dimension (EDD) between selected pairs of Runge-Kutta schemes across various nodal simulations for equilibrium position (0,0).

X ₀₀ =0, Y ₀₀ =0										
NODES										
	11 X 11	21 X 21	31 X 31	41 X 41	51 X 51	61 X 61	71 X 71	81 X 81	91 X 91	101 X 101
PAIR OF SCHEMES	SLOPE AND INTERCEPT									
RK2 - RK3	0.9007	0.8568	0.8644	0.8568	0.8701	0.8633	0.8595	0.8555	0.8500	0.8581
	0.0299	0.0984	0.0522	0.0840	0.0603	0.0644	0.0658	0.0709	0.0678	0.0726
RK2 - RK4	0.8991	0.8513	0.8721	0.8620	0.8617	0.8605	0.8652	0.8635	0.8544	0.8570
	0.0679	0.0926	0.0522	0.0791	0.0595	0.0644	0.0725	0.0656	0.0638	0.0692
RK2 - RK5	0.8975	0.8736	0.8415	0.8619	0.8629	0.8523	0.8595	0.8636	0.8567	0.8598
	0.0568	0.0711	0.0669	0.0744	0.0662	0.0715	0.0725	0.0665	0.0681	0.0699
RK2 - RK5M	0.9283	0.8732	0.8506	0.8571	0.8640	0.8476	0.8502	0.8639	0.8585	0.8555
	0.0372	0.0754	0.0588	0.0768	0.0611	0.0654	0.0749	0.0685	0.0652	0.0677
RK3 - RK4	0.9619	0.9286	0.9454	0.9390	0.9291	0.9360	0.9324	0.9370	0.9293	0.9295
	0.0582	0.0378	0.0401	0.0378	0.0389	0.0369	0.0532	0.0400	0.0437	0.0408
RK3 - RK5	0.9369	0.8966	0.9124	0.9110	0.9059	0.9091	0.9082	0.9146	0.9030	0.9043
	0.0622	0.0520	0.055	0.0510	0.0612	0.0557	0.0647	0.0551	0.0622	0.0593
RK3 - RK5M	0.9185	0.8855	0.9057	0.9016	0.9041	0.8952	0.9016	0.9169	0.9017	0.9036
	0.0756	0.0633	0.0574	0.0564	0.0580	0.0554	0.0651	0.0559	0.0653	0.0547
RK4 - RK5	0.9194	0.9601	0.9075	0.9095	0.9222	0.9117	0.9088	0.9110	0.9090	0.9102
	0.0427	0.0542	0.0534	0.0533	0.0567	0.0575	0.0548	0.0574	0.0633	0.0593
RK4 - RK5M	0.9013	0.8963	0.8983	0.9007	0.9118	0.8975	0.9013	0.9114	0.9055	0.9080
	0.0565	0.0646	0.0574	0.0583	0.0588	0.0574	0.0559	0.0593	0.0638	0.0556
RK5 - RK5M	0.9093	0.9209	0.9286	0.9339	0.9324	0.9260	0.9285	0.9407	0.9326	0.9340
	0.0622	0.0549	0.0435	0.0415	0.0388	0.0379	0.0419	0.0398	0.0412	0.0368

Table IX: Correlation Analysis of Pairs of Runge-Kutta schemes at 10,201 simulations for the three equilibrium positions.

INITIAL CONDITION	X ₀₀ =0, Y ₀₀ = -1	X ₀₀ =0, Y ₀₀ =0	X ₀₀ =0, Y ₀₀ =1
101 X 101 NODES			
PAIR OF SCHEMES	SLOPE AND INTERCEPT		
RK2 - RK3	0.8278	0.8581	0.8006
	0.0974	0.0726	0.1120
RK2 - RK4	0.8249	0.8570	0.8032
	0.0967	0.0692	0.1076
RK2 - RK5	0.8203	0.8598	0.8026
	0.1003	0.0699	0.1140
RK2 - RK5M	0.8246	0.8555	0.7969
	0.0975	0.0677	0.1150
RK3 - RK4	0.9056	0.9295	0.8991
	0.0600	0.0408	0.0665
RK3 - RK5	0.8685	0.9043	0.8592
	0.0851	0.0593	0.0997
RK3 - RK5M	0.8741	0.9036	0.8529
	0.0816	0.0547	0.1009
RK4 - RK5	0.8716	0.9102	0.8565
	0.0854	0.0593	0.1037
RK4 - RK5M	0.8709	0.9080	0.8563
	0.0860	0.0556	0.1008
RK5 - RK5M	0.9340	0.9340	0.9049
	0.0368	0.0368	0.0623

The dimension distribution summarized in figures 6 and 7 shows that there is a qualitative agreement of the estimated fractal disk dimension distribution for all schemes. The quantitative differences which were noted in figures 6 and 7 can be accounted for by the computational differences among the schemes.

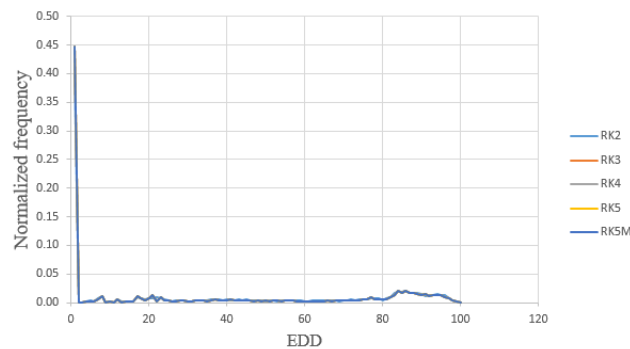


Figure 6: Normalized Frequency Distribution of the Estimated Fractal Disk Dimension (EDD) of Poincare Sections with constant simulation time step using all schemes with Damping coefficient ($0.0168 \leq \gamma \leq 0.1680$) and Excitation Amplitude ($0.10 \leq P_0 \leq 0.21$) at 101 by 101 simulation for equilibrium position (0,0).

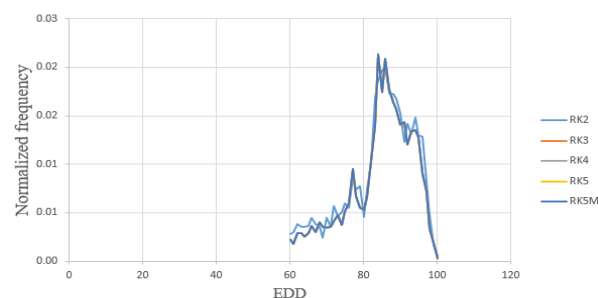


Figure 7: Zoomed-Up Normalized Frequency Distribution of the Estimated Fractal Disk Dimension (EDD) of Poincare Sections with constant simulation time step using all schemes with Damping coefficient ($0.0168 \leq \gamma \leq 0.1680$) and Excitation Amplitude ($0.10 \leq P_0 \leq 0.21$) at 101 by 101 simulation for equilibrium position (0,0).

VII. CONCLUSIONS AND RECOMMENDATIONS

The Poincare solutions and chaos diagrams obtained in this study compare very well with that of literature. Likewise fractal dimensions obtained across different schemes do not vary significantly quantitatively for corresponding nodes suggesting qualitative agreement of Poincare solutions. Furthermore, the study has shown that more than fifty percent of the studied parameters nodes drove the Duffing oscillator chaotically across equilibrium positions and Runge-Kutta schemes. In order to have a better and finer solution quickly, a faster computer better than (HP pavilion g6 Intel(R) Pentium(R) CPU 2020M @2.40GHz) that can handle higher resolution than 101 x 101 is highly recommended.

REFERENCES

- [1]. Jun, Y., Zhi-kun, X., and LiXian Y. 2008. Complex dynamics in a Duffing-van der pol oscillator with $\Phi 6$ Potential. Journal of the Physical Society of Japan 77(11).
- [2]. Zeeman, E. C. (2000, March 31). Duffing Equation: Catastrophic Jumps of Amplitude and Phase. Lecture presented at Trinity University.
- [3]. Liew, H. H. and Pan, Y. F. 2010. A Numerical Study of Ship's Rolling Motion. Proceedings of the 6th IMT-GT Conference on Mathematics, Statistics and its Applications. UniversitiTunku Abdul Rahman, Kuala Lumpur, Malaysia.
- [4]. Varsha, S. K. 2013. Complexity, Chaos, and the Duffing-Oscillator Model: An Analysis of Inventory Fluctuations in Markets. Journal of Applied Nonlinear Dynamics 3(2):147-158.
- [5]. Dowell, E.H. 1988. Chaotic Oscillations in Mechanical Systems. Computational Mechanics 3(1): 199-216.
- [6]. Salau, T.A.O. and Ajide, O.O. 2012. Comparative Analysis of Numerically Computed Chaos Diagrams in Duffing Oscillator. Journal of Mechanical Engineering and Automation 2(4): 53-57.
- [7]. Salau, T.A.O. and Ajide, O.O. 2013. Fractal Characterization and Comparison of Chaos Impact of Excited Duffing Oscillator Parameters. International Journal of Engineering Science and Technology 5(3): 547-554.
- [8]. Francis C. M. (1987), Chaotic Vibrations-An Introduction for Applied Scientists and Engineers, John Wiley & Sons, New York, ISBN 0-471-85685-1.
- [9]. Narayanan S. and Jayaraman K. (1989), Control of Chaotic Oscillations by Vibration Absorber. ASME Design Technical Conference, 12th Biennial Conference on Mechanical Vibration and Noise. DE 18.5, 391-394.
- [10]. Salau, T.A.O. and Ajide, O.O.2012. Fractal Characterization of evolving Trajectories of Duffing Oscillator. International Journal of Advances in Engineering & Technology Research (IAET).2(1):62-72.

Author's profile:

Dr. Salau Tajudeen Abiola Ogunniyi is a senior lecturer in the department of Mechanical Engineering, University of Ibadan, Nigeria. He was appointed by the University of Ibadan in February 1993 as Lecturer-II. By dint of hard work and his outstanding service contributions to the department, he was promoted to position of Lecturer-I in 2002 and Senior Lecturer in 2008. He had served the department in various capacities. He was the coordinator of the department for 2004/2005 and 2005/2006 academic sessions. He was the recipient of M.K.O Abiola postgraduate scholarship in 1993/94 academic session while on his Ph.D research programme at the University of Ibadan, Nigeria. Salau has many publications in scholarly journals and conference proceedings. His keen area of specialization is solid mechanics with bias in nonlinear dynamics (Chaos systems modelling and Fractal Characterisation). Salau is a corporate member, Nigerian Society of Engineers (NSE) and a registered Engineer by Council for Regulations of Engineering in Nigeria (COREN). He is happily married and blessed with children.

Olopade Taiwo Israelis is a graduate (2015/2016 academic session) of the department of Mechanical Engineering, University of Ibadan, Nigeria. He is a graduate member of the Nigerian Society of Engineers and he's also a 2012 recipient of the Mobile Telecommunication Network (MTN) foundation scholarship merit award.